Nine-vertex Polyhedral Monocarbaplatinaborane Chemistry. Isolation, Molecular Structure and Nuclear Magnetic Resonance Properties of [6,6-$(PPh_3)_2$-*arachno*-6,4-$PtCB_7H_{11}$] *

Jane H. Jones,[a] Bohumil Štíbr,[b] John D. Kennedy,[a] Andrew D. Lawrence[a] and Mark Thornton-Pett[a]

[a] *School of Chemistry, University of Leeds, Leeds LS2 9JT, UK*

[b] *Institute of Inorganic Chemistry, The Academy of Sciences of the Czech Republic, 25068 Řež u Prahy, The Czech Republic*

Reaction between [$Pt(PPh_3)_4$] and *nido*-1-CB_8H_{12} **1** results in the formation of [6,6-$(PPh_3)_2$-*arachno*-6,4-$PtCB_7H_{11}$] **2** as a yellow crystalline solid in 26% yield. The product **2** is characterised by NMR spectroscopy and single-crystal X-ray diffraction analysis. Crystals (from CH_2Cl_2–hexane) are triclinic, space group $P\bar{1}$, with a = 974.3(2), b = 1237.5(2), c = 1771.3(3) pm, α = 95.26(1), β = 95.43(1), γ = 110.10(1)° and Z = 2. The structure has been refined to $R(R')$ = 0.0256 (0.0394) for 6324 reflections [$F_o > 2.0\sigma(F_o)$]. The molecular structure is based on a nine-vertex *arachno* cluster with the platinum and carbon atoms in projecting open face 6- and 4-positions respectively. The ^{11}B, ^1H and ^{31}P NMR parameters have been measured and assigned to structural positions, and the ^{11}B and ^1H shielding patterns are compared to those of the related non-platinum species *arachno*-4,5-$C_2B_7H_{13}$ **7** and *arachno*-4,6-$C_2B_7H_{13}$ **8**. Incidental to this work the previously unreported ^1H shielding behaviour of the carbaboranes **1**, **7** and **8** have also been measured and assigned.

Although dicarbaborane chemistry is relatively well examined,[1-3] monocarbaborane chemistry is still in a number of respects yet in its infancy, and there is much chemistry to develop.[3] The neutral *nido* nine-vertex monocarbaborane *nido*-1-CB_8H_{12} **1**,[4,5] prepared from the thermolysis of *arachno*-4-CB_8H_{14},[5,6] is of interest because it does not have its carbon atom in an open-face site, a feature that is probably due to a tendency to preserve the [*nido*-B_9H_{12}]$^-$ type of hydrogen bridging system,[7] assisted by a preference for carbon to occupy an apical position that has lower connectivity.[7,8] As part of an approach to metallaheteroborane chemistry involving the oxidative insertion of platinum(0) species such as [$Pt(PPh_3)_4$] into heteroborane substrates,[9] we report herein the reaction of [$Pt(PPh_3)_4$] with *nido*-1-CB_8H_{12} **1** and the identification and characterisation of the metallamonocarbaborane product [6,6-$(PPh_3)_2$-*arachno*-6,4-$PtCB_7H_{11}$] **2**. This species is of some interest because nine-vertex *arachno* metallaboranes and metallacarbaboranes are quite rare.[9-13] The numbering systems for the nine-vertex *nido*, nine-vertex *arachno*, and ten-vertex *nido*–*arachno* clusters encountered in this work are shown in structures **I**, **II** and **III** respectively. Note that changes among these cluster types, and changes in cluster constituent, will alter the formal numbering of particular atoms.

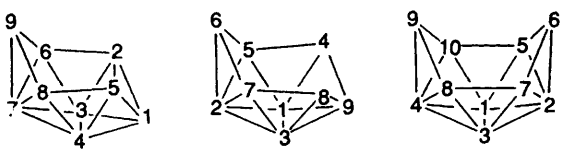

I II III

* *Supplementary data available:* see Instructions for Authors, *J. Chem. Soc., Dalton Trans.*, 1993, Issue 1, pp. xxiii–xxviii.

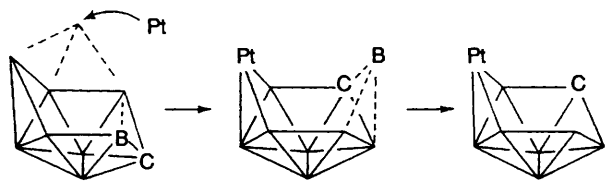

Scheme 1

Results and Discussion

Preparation of [6,6-$(PPh_3)_2$-*arachno*-6,4-$PtCB_7H_{11}$] **2**.—Reaction between *nido*-1-CB_8H_{12} **1** (schematic cluster structure **IV**) and [$Pt(PPh_3)_4$] in CH_2Cl_2 solution for 15 h at room temperature, followed by chromatographic separation of the reaction mixture, yielded a yellow crystalline air-stable solid in 26% yield. This was identified as [6,6-$(PPh_3)_2$-*arachno*-6,4-$PtCB_7H_{11}$] **2** (schematic cluster structure **V**) as described below, and was the only metallacarbaborane product in a quantity viable enough for reasonable characterisation (reaction scale 150 μmol). The reaction involves boron-vertex loss, and thereby has some geometric similarities to the reaction of the [*nido*-B_9H_{12}]$^-$ anion with [$PtCl_2(PMe_2Ph)_2$], which is believed to proceed *via* attack at the 2,6,9 positions by the platinum centre, accompanied by the loss of the B(5) vertex and cluster opening.[14,15] An exactly analogous reaction geometry would account for the cluster constituent positions in the product **2** described here (Scheme 1).

Thus it is reasonable to suggest that 1-CB_8H_{12} and [$Pt(PPh_3)_4$] initially form a ten-vertex [9,9-$(PPh_3)_2$-*arachno*-9,5-$PtCB_8H_{12}$] type of intermediate of configuration **VI** (see also Scheme 1). This would be unstable because of the cage carbon at the high-connectivity C(5) position,[8,16] and loss of the B(6) vertex, probably with nucleophilic assistance from liberated PPh_3 or fortuitous moisture, would then lead directly to compound **2** with the cage carbon in the more stable open-face C(4) position as in structure **V**.

Table 1 Selected interatomic distances (pm) for [6,6-$(PPh_3)_2$-*arachno*-4,6-$PtCB_7H_{11}$] **2** with estimated standard deviations (e.s.d.s) in parentheses

P(1)–Pt(6)	233.0(3)	P(2)–Pt(6)	232.2(3)
B(2)–Pt(6)	221.4(8)		
B(5)–Pt(6)	221.0(8)	B(7)–Pt(6)	220.3(8)
C(111)–P(1)	183.2(5)	C(211)–P(2)	184.9(5)
C(121)–P(1)	184.1(5)	C(221)–P(2)	181.6(5)
C(131)–P(1)	184.7(5)	C(231)–P(2)	183.1(5)
B(2)–B(1)	174.0(11)	B(3)–B(2)	178.7(12)
B(3)–B(1)	175.9(13)		
C(4)–B(1)	167.3(13)	B(8)–B(3)	168.7(14)
B(5)–B(1)	174.2(12)	B(7)–B(3)	175.2(11)
B(9)–B(1)	182.5(14)	B(9)–B(3)	181.3(12)
B(5)–B(2)	175.2(12)	B(7)–B(2)	175.6(12)
B(5)–C(4)	173.1(13)	B(8)–B(7)	179.7(14)
B(9)–C(4)	168.1(13)	B(9)–B(8)	177.6(15)
H(1)–B(1)	105(7)	H(3)–B(3)	106(7)
H(2)–B(2)	109(6)	H(9)–B(9)	113(7)
H(4a)–C(4)	98(9)	H(4b)–C(4)	121(8)
H(78)–B(7)	140(9)	H(78)–B(8)	112(9)
H(89)–B(8)	110(7)	H(89)–B(9)	147(7)
H(5)–B(5)	113(8)	H(7)–B(7)	110(9)
H(8)–B(8)	110(8)		

Table 2 Selected angles (°) between interatomic vectors for [6,6-$(PPh_3)_2$-*arachno*-4,6-$PtCB_7H_{11}$] **2** with e.s.d.s in parentheses

P(2)–Pt(6)–P(1)	100.0(1)		
B(2)–Pt(6)–P(1)	128.0(3)	B(2)–Pt(6)–P(2)	130.2(2)
B(5)–Pt(6)–P(1)	84.9(3)	B(7)–Pt(6)–P(2)	89.7(3)
B(7)–Pt(6)–P(1)	165.4(2)	B(5)–Pt(6)–P(2)	173.2(2)
B(5)–Pt(6)–B(2)	46.7(3)	B(7)–Pt(6)–B(2)	46.8(3)
B(7)–Pt(6)–B(5)	84.7(4)		
B(5)–C(4)–B(1)	61.5(5)	B(7)–B(8)–B(3)	60.3(5)
B(9)–C(4)–B(1)	65.9(6)	B(9)–B(8)–B(3)	63.1(6)
B(9)–C(4)–B(5)	114(6)	B(9)–B(8)–B(7)	106.2(7)
H(4a)–C(4)–B(1)	123(5)	H(78)–B(8)–B(3)	107(5)
H(4a)–C(4)–B(5)	118(5)	H(78)–B(8)–B(7)	51(5)
H(4a)–C(4)–B(9)	124(5)	H(78)–B(8)–B(9)	114(5)
H(4b)–C(4)–B(1)	127(4)	H(89)–B(8)–B(3)	115(4)
H(4b)–C(4)–B(5)	82(4)	H(89)–B(8)–B(7)	118(4)
H(4b)–C(4)–B(9)	101(4)	H(89)–B(8)–B(9)	56(4)
H(4b)–C(4)–H(4a)	108(6)	H(89)–B(8)–H(78)	81(5)
C(4)–B(5)–Pt(6)	111.1(6)	B(8)–B(7)–Pt(6)	116.0(6)
B(8)–B(9)–C(4)	121.1(7)		
H(89)–B(9)–C(4)	102(3)	H(89)–B(9)–B(8)	38(3)
B(8)–H(78)–B(7)	90(6)	B(9)–H(89)–B(8)	86(5)

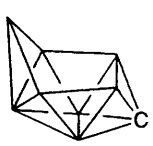

IV

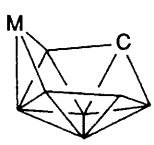

V

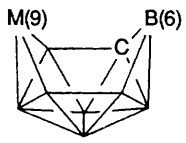

VI

Molecular Structure of [6,6-$(PPh_3)_2$-*arachno*-6,4-$PtCB_7H_{11}$] **2**.—Crystals suitable for single-crystal X-ray diffraction analysis were grown by allowing hexane to diffuse into a solution of compound **2** in dichloromethane. The diffraction measurements were made at 200 K (see Experimental section for details), and the data set obtained was of good quality, which enabled the ready and unambiguous location of all hydrogen atoms associated with the cluster. Selected interatomic distances and angles are in Tables 1 and 2 respectively. The molecular structure is shown in Fig. 1.

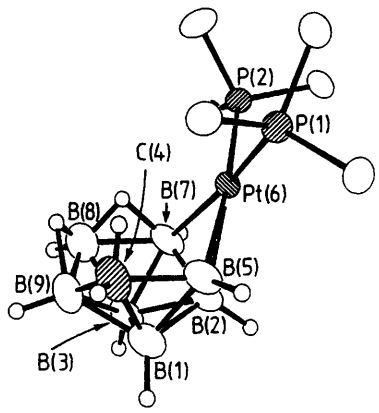

Fig. 1 Molecular structure of [6,6-$(PPh_3)_2$-*arachno*-6,4-$PtCB_7H_{11}$] **2**, with phenyl atoms (apart from the *ipso* carbons) omitted for clarity

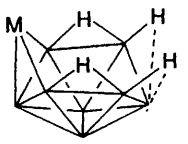

VII

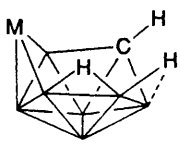

VIII

The cluster structure is readily seen to be that of an *arachno* nine-vertex species (structure **II**),[8,16] with the platinum and carbon atoms in the projecting open-face 6- and 4-positions. As such the cluster structure is similar to those of the previously reported *arachno* nine-vertex eight-boron species [$(PMe_2Ph)_2$-PtB_8H_{12}] **3**,[14,15,17] [(CO)H$(PMe_3)_2IrB_8H_{11}Cl$] **4**,[18] and [$(\eta^5$-$C_5Me_5)$(MeNC)IrB_8H_{12}] **5**,[19] all of schematic structure **VII**, the difference being that the {BH_2} group at the 4-position of these eight-boron species, together with the adjacent 4,5-bridging hydrogen atom (numbering, for convenience of comparison, as in Fig. 1), have been notionally replaced by an isoelectronic {CH_2} group in the new {$PtCB_7$} species **2** reported here (schematic structure **VIII**).

In this context it is useful to examine the changes in geometry that are associated with the bridging and *endo* hydrogen atoms when the eight-boron species, as best typified by [$(\eta^5$-$C_5Me_5)$(MeNC)IrB_8H_{12}],[19] and the one-carbon seven-boron compound [6,6-$(PPh_3)_2$-*arachno*-6,4-$PtCB_7H_{11}$] **2** are compared.

The principal differences arise from the reluctance of the carbon atom to form C–H–B bridges.[8,16] These differences occur around the 4 position (see Fig. 1 and structures **II**, **VII** and **VIII**). In compound **2** the {CH_2} group has one *exo* hydrogen atom, and one *endo* hydrogen atom that exhibits no bridging character. Thus the H(4)(*endo*)–C(4) angles to C(4)–B(5) and C(4)–B(9) are 82(4) and 101(4)° respectively, and the H(4)(*exo*)–C(4)–H(4)(*endo*) angle approximates to tetrahedral at 108(6)°. This contrasts to the {IrB_8H_{12}} species **5** (structure **VII**) where B(4) has, in addition to its *exo* hydrogen atom, two hydrogen bridges, one to each of its two adjacent boron atoms on the open face [these are also exhibited by the equivalent B(8) position]. In this {IrB_8} species each of these hydrogen bridges is asymmetric. Those in the 4,5- and 7,8-positions show weaker bonding (by about 10–15 pm) to the boron atoms B(5) and B(7) adjacent to the metal site, and stronger bonding to the projecting B(4) and B(8) atoms. This feature is mirrored by the 7,8 hydrogen in the {$PtCB_7$} species **2**. The bridging hydrogen atoms in the 4,9- and 8,9-positions in the {IrB_8} species **5** also show stronger bonding to these B(4) and B(8) positions, with much weaker interaction (by about 50 pm) towards the central B(9) atom. In the {$PtCB_7$} species **2** this latter bridge asymmetry is not nearly so marked, however, the difference dropping to *ca.* 25 pm. Presumably the lack of a bridge bond to C(4) releases more bonding character for the B(9)–H(8,9) linkage in this case.

Table 3 Measured NMR parameters for [6,6-$(PPh_3)_2$-*arachno*-6,4-$PtCB_7H_{11}$] **2** in $CDCl_3$ solution at 294–297 K[a]

Assignment	δ(^{11}B)	$w_{\frac{1}{2}}$/Hz	δ(^{1}H)	Observed [^{1}H–^{1}H]-COSY correlations[b,c]
2	+19.1	350	+4.27	—
9	+9.3	420	+3.42	—
5	+1.5[d]	*ca.* 220	+2.57	—
7	+0.1[e]	*ca.* 350	+2.89	2m μ-7,8w
1	−9.7	280	+1.99[h]	*endo* 4s μ-7,8s μ-8,9w
8	−17.8	280	+1.98[h]	
3	−43.8	110	−0.03[f]	5m
4	[CH]	—	+0.08 (*exo*)	*endo* 4s
			−1.25 (*endo*)	*exo* 4s
μ-7,8	—	—	−1.65[g]	*exo* 4w 3,6s μ-8,9m
μ-6,7	—	—	−2.30[h]	3,6w μ-7,8m

[a] Additional data: δ(^{31}P) +27.8 [^1J(^{195}Pt–^{31}P) 2770] and +29.3 [^1J(^{195}Pt–^{31}P) 2894, ^2J(^{31}P–^{31}P) 12 Hz]. [b] Note δ(^{1}H) for 3 and 6 positions accidentally the same. [c] Measured under conditions of complete {^{11}B(broad-band noise)} decoupling; s = strong, w = weak, m = intermediate. [d] ^1J(^{195}Pt–^{11}B) *ca.* 280 Hz. [e] Possible satellites, ^1J(^{195}Pt–^{11}B) *ca.* 300 Hz. [f] Satellites arising from ^3J(^{195}Pt–^{1}H) 66 Hz. [g] Sharpened selectively by ν(^{11}B) corresponding to δ(^{11}B) +0.1 and −17.8. [h] Sharpened selectively by ν(^{11}B) corresponding to δ(^{11}B) +9.3 and −17.8.

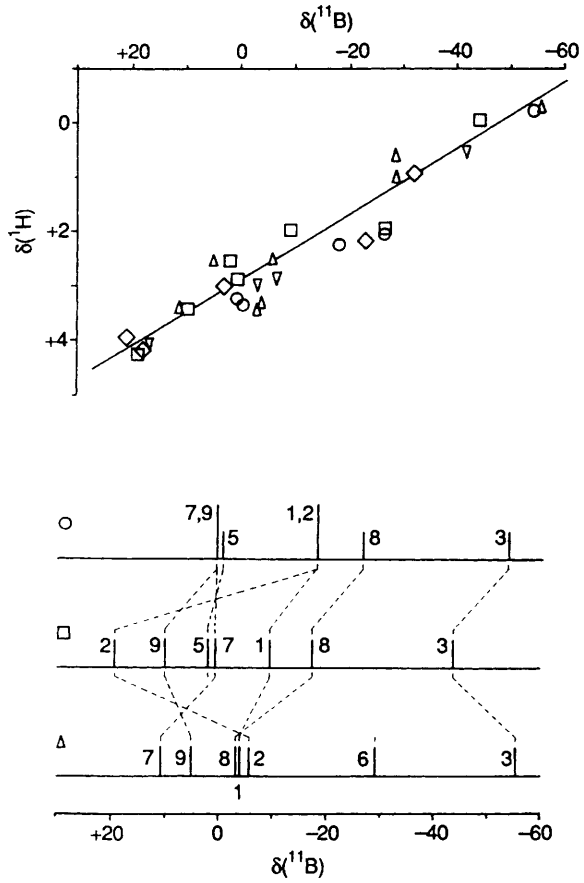

Fig. 2 Nuclear magnetic resonance data for [6,6-$(PPh_3)_2$-*arachno*-6,4-$PtCB_7H_{11}$] **2** (□), together with those for *arachno*-4,6-$C_2B_7H_{13}$ **8** (○) and *arachno*-4,5-$C_2B_7H_{13}$ **7** (△) for comparison. The top diagram plots δ(^{1}H) *versus* δ(^{11}B) for BH(exo) units, and also includes data for *arachno*-4-CB_8H_{14} **6** (▽) and [$(PMe_2Ph)_2PtB_8H_{12}$] **3** (◇). The line drawn has slope δ(^{11}B):δ(^{1}H) 16.5:1, intercept +2.8 in δ(^{1}H). The bottom diagrams are stick representations of the chemical shifts and relative intensities in the ^{11}B spectra. Of these, the top two diagrams demonstrate the effect of replacing the {$C(6)H_2$} unit in *arachno*-4,6-$C_2B_7H_{13}$ **8** by {$(PPh_3)_2Pt$} to generate [6,6-$(PPh_3)_2$-*arachno*-6,4-$PtCB_7H_{11}$] **2**. The bottom two show the effect of replacing {$B(6)H_2$} and {$C(5)H$}$^+$ units in 4,5-$C_2B_7H_{13}$ **7** by {$(PPh_3)_2Pt$}$^+$ and {BH} respectively, also to give **2**. The hatched lines drawn connect equivalent positions in the three compounds

The interboron and boron–carbon distances in compound **2** are all within typical ranges, with the smaller carbon atom and its *endo* terminal hydrogen [as distinct from B(8) and its two bridging hydrogen atoms] introducing the obvious departure from the effective mirror-plane symmetry of the all-boron analogue **5** (structure **VII**). The effect of the C(4) centre in **2** is also reflected in significant differences in interboron distances, as compared to the {IrB_8H_{12}} species **5**, throughout the cluster. However, this asymmetry does not seem to be carried through to any significant extent to the bonding about platinum, with the distances from Pt(6) to B(5) and B(7) being essentially identical within experimental error, a feature also of Pt(6)–P(1) and Pt(6)–P(2). This is also reflected in the small difference between the two ^1J(^{195}Pt–^{31}P) values obtained by NMR spectroscopy (Table 3). There is also only a small twist between the Pt(6)P(1)P(2) and Pt(6)B(5)B(7) planes, of 11.7(2)°.

The crystal selected for the diffraction analysis contained 0.25 molecule of benzene per molecule of compound. The origin of this molecule is not apparent since benzene itself was not deliberately used during the synthesis or crystallisation (see Experimental section). An interesting possible source could be from one of the PPh_3 ligands shed from the labile [$Pt(PPh_3)_4$] starting material. A PPh_3 phenyl-group cleavage does have some precedent in the reported[20] action of acetylene with [$(PPh_3)(PhPC_6H_4)HIrB_9H_{12}$] at *ca.* 355 K, in which phenyl-stripped unsubstituted PH_3 phosphine ligands are co-ordinated to the metal atom of the metallaborane product.[20] The present conditions are however much milder, and it seems more reasonable that in this case the benzene arises from a fortuitous contamination in the crystallisation experiments.

Nuclear Magnetic Resonance Studies.—The measured NMR parameters for [6,6-$(PPh_3)_2$-*arachno*-6,4-$PtCB_7H_{11}$] **2** are given in Table 3, and selected features, together with other data for comparison, are presented in Fig. 2. The parameters are entirely in accord with the molecular structure discussed above, confirming that the crystal selected was representative of the bulk sample. Seven different ^{11}B resonance positions were apparent, and ^{1}H together with ^{1}H-{^{11}B(selective)} spectroscopy distinguished all the cluster ^{1}H resonance positions, and related them to their corresponding ^{11}B resonances, thus permitting a partial assignment of the spectra. The ^{11}B linewidths were too great for successful [^{11}B–^{11}B]-COSY experiments, but [^{1}H–^{1}H]-COSY–{^{11}B} experiments showed some interproton correlations that assisted further assignment, with the final assignments in Table 3 being supported also by the incidence of observed ^{11}B and ^{1}H couplings to ^{195}Pt and the site-specific features of typical[17–19,21,22] nine-vertex *arachno* character. The ^{1}H shielding variations of **2** are found to parallel the ^{11}B shielding changes (Fig. 2, uppermost diagram), with the slope of the correlation parallelling those of other related *arachno* nine-vertex species such as [6,6-$(PMe_2Ph)_2$-*arachno*-6-

Table 4 Measured NMR parameters for *nido*-1-CB_8H_{12} **1** and $[nido\text{-}B_9H_{12}]^-$ at 294–297 K

	1-CB_8H_{12} in $CDCl_3$		$[NEt_4][B_9H_{12}]$ in CD_2Cl_2[a]	
Assignment	$\delta(^{11}B)$	$\delta(^1H)$	$\delta(^{11}B)$	$\delta(^1H)$
9	+7.6	+4.11	−14.5	+2.60
3,4	−3.3	+2.67	−10.0	+1.68
6,8	−11.5	+2.27	−13.9	+1.72
2,5	−26.5	+1.99, −5.05	−34.2	+0.71, −7.14
7	−53.3	−0.28	−52.0	−0.94
1	[CH]	+4.10	−10.0	+2.72
μ-6,9; 8,9	—	−2.71	—	−2.96

[a] Data from ref. 24.

Table 5 Measured ^1H and ^{11}B NMR chemical shifts for *arachno*-4,5-$C_2B_7H_{13}$ **7** and *arachno*-4,6-$C_2B_7H_{13}$ **8** in CD_2Cl_2 solution at 294–297 K[a]

	Compound **7**		Compound **8**	
Assignment[a]	$\delta(^{11}B)$	$\delta(^1H)$	$\delta(^{11}B)$	$\delta(^1H)$
1	−3.9	+3.31	−18.1	+2.23
2	−5.3[b]	+2.49		
3	−55.6	−0.28	−53.4	−0.20
4	$[CH_2]$	+1.64 (2 H)[c]	$[CH_2]$	+0.22, −0.78
6	−29.2	+0.98, +0.56		
5	[CH]	+2.51	−0.6	+3.35
7	+10.7[d]	+3.44	0.0	+3.23
9	+5.0	+2.52		
8	−3.1[e]	+3.42	−26.7	+2.62
μ-7,8	—	−1.42	—	−1.40
μ-8,9	—	−1.18		

[a] For assignments see ref. 27. [b] Coupling $^1J(^{11}B\text{–}^{11}B)$ *ca.* 27 Hz apparent. [c] *exo* and *endo* ^1H resonances accidentally coincident in this solvent. [d] Coupling $^1J(^{11}B\text{–}^{11}B)$ *ca.* 38 Hz apparent. [e] Coupling $^1J(^{11}B\text{–}^{11}B)$ *ca.* 22 Hz apparent.

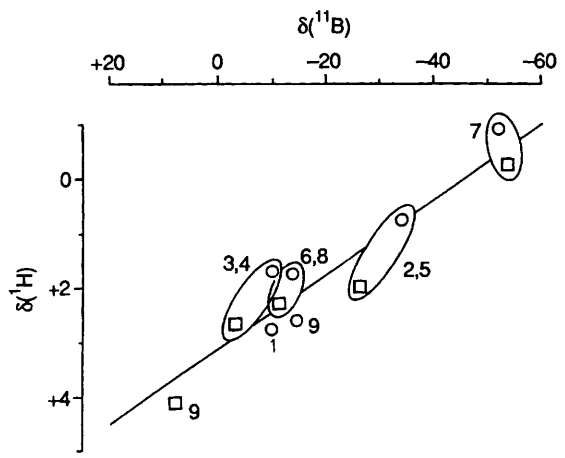

Fig. 3 Plot of $\delta(^1H)$ *versus* $\delta(^{11}B)$ for directly bound BH(*exo*) units in *nido*-1-CB_8H_{12} **1** (□) and $[nido\text{-}B_9H_{12}]^-$ (○). The line drawn has slope $\delta(^{11}B):\delta(^1H)$ 14:1, intercept +3.1 in $\delta(^1H)$

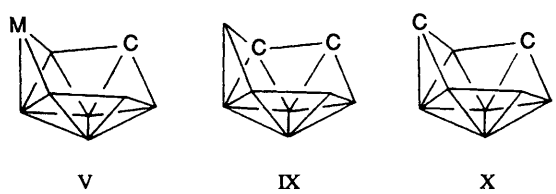

$PtB_8H_{12}]$ **3**,[15,17] as well as those of non-metalla analogues such as *arachno*-4-CB_8H_{14} **6**[23] and the isomeric pair of dicarbaboranes *arachno*-4,5-$C_2B_7H_{13}$ **7** and *arachno*-4,6-$C_2B_7H_{13}$ **8**. There is a general $\delta(^{11}B):\delta(^1H)$ correlation slope of *ca.* 16.5:1.

The bottom diagrams in Fig. 2 are stick representations of the ^{11}B chemical shifts and relative intensities for $[6,6\text{-}(PPh_3)_2\text{-}arachno\text{-}6,4\text{-}PtCB_7H_{11}]$ **2** and the structurally similar *arachno* dicarbaboranes 4,5-$C_2B_7H_{13}$ **7** and 4,6-$C_2B_7H_{13}$ **8**. The most straightforward carborane comparison for compound **2** is afforded by the dicarbaborane **8**. Here an isolobal replacement of the $\{CH_2\}$ unit in the 6 position of compound **8** (structure **X**) by a $\{Pt(PPh_3)_2\}$ unit leads directly to isostructural **2** (structure **V**) with no bridging hydrogen changes. This isostructurality is reflected in the close shielding parallels shown in Fig. 2 (lower section, upper two diagrams). These shielding changes are also mimicked when the 4,5-isomer of *arachno*-$C_2B_7H_{13}$, **7**, (structure **IX**) is compared to compound **2** (Fig. 2, lowest two diagrams), again confirming the close structural and bonding parallels. In this last case it is the $\{BH_2\}$ unit in the 6 position that is notionally replaced by isolobal and isoelectronic $\{Pt(PPh_3)_2\}^+$, and there is a compensating change from $\{CH\}^+$ to its isolobal and isoelectronic equivalent $\{BH\}$ in the 5-position (*cf.* structures **V** and **IX**). Again there are no bridging hydrogen changes. In both comparisons the only particularly marked change is for the non-open-face B(2) position adjacent to the platinum centre, a phenomenon in *arachno* nine- and ten-vertex clusters that has been noted and adequately discussed elsewhere.[17,24,25]

A final NMR comparison for compound **2** is that for the coupling constants $^1J(^{195}Pt\text{-}^{31}P)$. The values for $[(PMe_2Ph)_2\text{-}PtB_8H_{12}]$ **3** (2724 Hz)[17] and compound **2** (2770 and 2894, average 2832 Hz) are very similar, the larger value for compound **2** possibly reflecting a marginally greater electronegativity or pd electron demand by the $\{CB_7H_{11}\}$ *versus* the $\{B_8H_{12}\}$ fragment.

Other new NMR measurements implicit in the above discussion are those of the proton shieldings of the nine-vertex *nido*-1-CB_8H_{12} starting material **1** (Table 4) and of the arachno nine-vertex dicarbaborane isomeric pair 4,5-$C_2B_7H_{13}$ **7** and 4,6-$C_2B_7H_{13}$ **8** (Table 5). The ^{11}B shifts and assignments have been reported and discussed previously,[7,21,22,26,27] but no proton work has been described. For present purposes, the proton shieldings of the two *arachno* species **7** and **8** are adequately dealt with above and in Fig. 2.

Table 6 Non-hydrogen and cluster-hydrogen fractional atomic coordinates ($\times 10^4$) for [6,6-$(PPh_3)_2$-*arachno*-4,6-$PtCB_7H_{11}$] **2** with e.s.d.s in parentheses

Atom	*x*	*y*	*z*	Atom	*x*	*y*	*z*
Pt(6)	3110.3(2)	1086.1(2)	2627.5(1)	C(211)	2860(3)	2185(3)	4575(2)
P(1)	4478(2)	2181(1)	1771(1)	C(212)	3774(3)	2268(3)	5250(2)
P(2)	3575(1)	2519(1)	3660(1)	C(213)	3164(3)	2002(3)	5921(2)
B(1)	1988(9)	−1784(6)	2024(5)	C(214)	1641(3)	1653(3)	5918(2)
B(2)	1412(7)	−679(5)	2386(4)	C(215)	728(3)	1571(3)	5242(2)
B(3)	1658(8)	−1704(6)	2983(5)	C(216)	1337(3)	1837(3)	4571(2)
C(4)	3804(9)	−1206(7)	1995(5)	C(221)	2754(4)	3594(3)	3461(2)
B(5)	2718(9)	−409(6)	1745(4)	C(222)	3114(4)	4641(3)	3938(2)
B(7)	2122(8)	−245(6)	3358(4)	C(223)	2409(4)	5417(3)	3774(2)
B(8)	3190(12)	−1111(8)	3629(6)	C(224)	1344(4)	5147(3)	3134(2)
B(9)	3358(8)	−1880(6)	2766(5)	C(225)	984(4)	4100(3)	2656(2)
C(111)	3423(4)	2163(3)	854(2)	C(226)	1689(4)	3324(3)	2820(2)
C(112)	1896(4)	1595(3)	729(2)	C(231)	5570(3)	3208(3)	3941(2)
C(113)	1089(4)	1640(3)	47(2)	C(232)	6380(3)	4377(3)	3923(2)
C(114)	1809(4)	2254(3)	−511(2)	C(233)	7913(3)	4793(3)	4096(2)
C(115)	3335(4)	2822(3)	−386(2)	C(234)	8636(3)	4039(3)	4288(2)
C(116)	4142(4)	2776(3)	297(2)	C(235)	7826(3)	2870(3)	4306(2)
C(121)	5912(4)	1581(3)	1572(2)	C(236)	6293(3)	2454(3)	4133(2)
C(122)	6037(4)	1121(3)	844(2)	H(1)	1390(74)	−2470(60)	1595(39)
C(123)	7086(4)	603(3)	750(2)	H(2)	306(62)	−682(47)	2206(31)
C(124)	8009(4)	545(3)	1384(2)	H(3)	802(73)	−2370(58)	3180(37)
C(125)	7885(4)	1004(3)	2112(2)	H(4a)	4291(97)	−1476(76)	1595(51)
C(126)	6836(4)	1522(3)	2207(2)	H(4b)	4638(82)	−258(67)	2297(42)
C(131)	5525(4)	3758(2)	1974(2)	H(5)	2811(87)	−241(68)	1131(47)
C(132)	4714(4)	4491(2)	2022(2)	H(7)	1472(73)	−34(56)	3785(38)
C(133)	5440(4)	5692(2)	2150(2)	H(8)	3299(88)	−1439(71)	4180(48)
C(134)	6977(4)	6160(2)	2230(2)	H(9)	3641(71)	−2654(57)	2917(37)
C(135)	7788(4)	5426(2)	2182(2)	H(78)	3559(93)	−148(76)	3625(47)
C(136)	7062(4)	4225(2)	2054(2)	H(89)	4230(83)	−971(64)	3392(42)

For the *nido* species 1-CB_8H_{12} **1** a plot of $\delta(^1H)$ *versus* $\delta(^{11}B)$ for the {BH} units, together with equivalent data[28] for the anionic all-boron analogue [*nido*-B_9H_{12}]$^-$ for comparison, is given in Fig. 3. It can be seen that the ^1H shielding behaviour of the two species is very similar, with all ^{11}B,^1H points lying close to the same correlation line. In these terms the large antipodal shift for $^{11}B(9)$ in **1**, which has been commented upon elsewhere,[7,22] is not associated with any ^1H shielding anomaly. It may be noted that the value for the correlation slope $\delta(^{11}B):\delta(^1H)$ of *ca.* 14:1 is somewhat steeper than that of *ca.* 16.5:1 for the *arachno* species in Fig. 2, consistent with a more general observation that the $\delta(^{11}B):\delta(^1H)$ slope often decreases in the order *arachno* > *nido* > *closo* for otherwise closely related species.[25,29–34] An additional noteworthy feature is the high ^1H shielding at the bridging 2,5 position, a feature which is becoming characteristic of the nine-vertex *nido* system in boron-containing cluster chemistry.[28,30]

Experimental

General.—The samples of *nido*-1-CB_8H_{12} **1**,[6] [$Pt(PPh_3)_4$],[35] *arachno*-4-CB_8H_{14} **6**,[5,6] *arachno*-4,6-$C_2B_7H_{13}$ **8**[36] and *arachno*-4,5-$C_2B_7H_{13}$ **7**[37] were made by literature methods. NMR spectroscopy was performed as described in other recent papers from our laboratories,[38–40] with chemical shifts δ being given in ppm to high frequency (low field) of Ξ = 32.083 971 MHz [nominally $BF_3(OEt_2)$ in $CDCl_3$] for ^{11}B (quoted ±0.5 ppm), Ξ = 40.480 730 MHz (nominally 85% H_3PO_4) for ^{31}P (quoted ±0.5 ppm) and Ξ = 100 MHz ($SiMe_4$) for ^1H (quoted ±0.05 ppm), Ξ being defined as in ref. 41.

Preparation of [6,6-$(PPh_3)_2$-*arachno*-6,4-$PtCB_7H_{11}$] **2**.—The compound *nido*-7-CB_8H_{12} **1** (17 mg, 154 μmol) and [$Pt(PPh_3)_4$] (191 mg, 154 μmol) were stirred at room temperature in CH_2Cl_2 (15 cm^3) for 15 h. The reaction mixture remained yellow throughout. The mixture was filtered through silica gel (TLC grade) with the aid of more CH_2Cl_2 (*ca.* 20 cm^3). The resulting yellow filtrate was reduced to dryness (rotary evaporator, room temperature, water-pump pressure), redissolved in CH_2Cl_2–hexane (70:30, *ca.* 5 cm^3), and applied to preparative TLC plates [Silica (Fluka type GF 254), 200 × 200 × 1 mm on glass, prepared from a water slurry and dried at *ca.* 355 K in air]. Development with CH_2Cl_2–hexane (70:30) gave three yellow bands (R_f = 0.85, 0.60 and 0.20). Each of these was removed from the plate and extracted with CH_2Cl_2 (*ca.* 20 cm^3). Evaporation of the extract of the band at R_f 0.85 and repeated TLC gave a yellow microcrystalline solid, identified as [6,6-$(PPh_3)_2$-*arachno*-6,4-$PtCB_7H_{11}$] as described in the text (33 mg, 40 μmol, 26%). Crystals suitable for single-crystal X-ray diffraction analysis were grown by diffusion of hexane into a solution of the compound in CH_2Cl_2. Boron-11 NMR spectroscopy showed that the other two bands did not contain significant quantities of boron.

Single-crystal X-Ray Diffraction Analysis of Compound **2**.—The crystallography was carried out at 200.0 ± 0.1 K on a Stoe Stadi4 diffractometer using an ω–θ scan mode and graphite-monochromated Mo-Kα radiation (λ = 71.069 pm), and following a standard procedure.[42] The data set was corrected for absorption semi-empirically using azimuthal ψ-scans.[43] The structure was solved by standard Patterson (for the platinum atom) and Fourier difference techniques and was refined by full-matrix least squares using the SHELX 76 program system.[44] All non-hydrogen atoms were refined anisotropically with phenyl groups treated as rigid bodies with idealised hexagonal symmetry (C–C = 139.5 pm). All phenyl hydrogen atoms were included in calculated positions (C–H = 96 pm) and were assigned to an overall isotropic thermal parameter. The cluster hydrogen atoms were readily located from a Fourier difference synthesis, and were refined with individual isotropic thermal parameters. The total number of parameters was 409. The weighting scheme $w = [\sigma^2(F_o) + 0.0008\ (F_o)^2]^{-1}$ gave a satisfactory analysis of variance. Final atomic coordinates are in Table 6.

Crystal data. $C_9H_{20}B_9P_2Pt\cdot0.25C_6H_6$, M = 837.97 (includes benzene), triclinic, space group $P\bar{1}$, with a = 974.3(2), b = 1237.5(2), c = 1771.3(3) pm, α = 95.26(1), β = 95.43(1), and γ = 110.10(1); U = 1.9789(6) nm^3, Z = 2, D_c = 1.41 g cm^{-3}, μ(Mo-Kα) = 36.86 cm^{-1}, $F(000)$ = 842.97, $R(R')$ = 0.0256 (0.0394) for 6324 reflections with $F_o > 2.0\sigma(F_o)$, crystal dimensions 0.5 × 0.3 × 0.15.

Data collection. Scan speeds 1.5–8.0° min^{-1}, ω scan widths 1.05 + α-doublet splitting, range 4.0 < 2θ < 50°, 6964 data collected of which 6324 reflections with $F_o > 2.0\sigma(F_o)$ were considered observed.

Additional material available from the Cambridge Crystallographic Data Centre comprises H-atom coordinates, thermal parameters and remaining bond lengths and angles.

Acknowledgements

Contribution no. 29 from the Řež–Leeds Anglo–Czech Polyhedral Collaboration (ACPC). The authors thank the Royal Society, Borax Research Limited, the SERC and the Academy of Sciences of the Czech Republic for support, and Dr. T. Scott Griffin and Dr. Dana M. Wagnerová for their helpful cooperation. We also thank Professor N. N. Greenwood for his interest in the initial stages of this work.

References

1 R. N. Grimes, *Carboranes*, Academic Press, New York, 1970.
2 T. Onak in *Comprehensive Organometallic Chemistry*, eds. G. Wilkinson, F. G. A. Stone and E. Abel, Pergamon, Oxford, 1982, ch. 5.4.
3 B. Štíbr, *Chem. Rev.*, 1992, **92**, 225.
4 K. Baše, S. Heřmánek and B. Štíbr, *Chem. Ind. (London)*, 1977, 957.
5 K. Baše, B. Štíbr, J. Dolansky and J. Duben, *Collect. Czech. Chem. Commun.*, 1981, **46**, 245.
6 B. Štíbr, K. Baše, S. Heřmánek and J. Plešek, *J. Chem. Soc., Chem. Commun.*, 1976, 150.
7 S. Heřmánek, J. Fusek, B. Štíbr, J. Plešek and T. Jelínek, *Polyhedron*, 1986, **5**, 1873.
8 R. E. Williams, *Adv. Inorg. Chem. Radiochem.*, 1976, **18**, 67.
9 K. Baše, B. Štíbr, and I. A. Zakharova, *Synth. React. Inorg. Metal-Org. Chem.*, 1980, **10**, 509.
10 R. N. Grimes, in *Organometallic Reactions and Syntheses*, ed. E. I. Becker, Plenum, New York, 1977, vol. 6, pp. 63–214.
11 R. N. Grimes, in *Comprehensive Organometallic Chemistry*, eds. G. Wilkinson, F. G. A. Stone and E. Abel, Pergamon, Oxford, 1982, ch. 5.5.
12 J. D. Kennedy, *Prog. Inorg. Chem.*, 1986, **34**, 211.
13 See A. J. Welch, *Ann. Rep. Chem. Soc., Sect. A*, 1981–1983, **78–80**; R. Greatrex, *Ann. Rep. Chem. Soc., Sect. A*, 1984–1987, **81–84**; and M. A. Beckett, *Ann. Rep. Chem. Soc., Sect. A*, 1990–1991, **87**, 88 and following.
14 N. N. Greenwood, M. J. Hails, J. D. Kennedy and W. S. McDonald, *J. Chem. Soc., Dalton Trans.*, 1985, 953.
15 R. Ahmed, J. E. Crook, N. N. Greenwood and J. D. Kennedy, *J. Chem. Soc., Dalton Trans.*, 1986, 2433.
16 R. E. Williams, *Inorg. Chem.*, 1971, **10**, 210.
17 S. K. Boocock, N. N. Greenwood, M. J. Hails, J. D. Kennedy and W. S. McDonald, *J. Chem. Soc., Dalton Trans.*, 1981, 1415.
18 J. Bould, J. E. Crook, N. N. Greenwood and J. D. Kennedy, *J. Chem. Soc., Dalton Trans.*, 1984, 1903.
19 K. Nestor, X. L. R. Fontaine, N. N. Greenwood, J. D. Kennedy and M. Thornton-Pett, *J. Chem. Soc., Dalton Trans.*, 1989, 1465.
20 J. Bould, P. Brint, X. L. R. Fontaine, J. D. Kennedy and M. Thornton-Pett, *J. Chem. Soc., Chem. Commun.*, 1989, 1763; J. Bould, P. Brint, J. D. Kennedy and M. Thornton-Pett, *J. Chem. Soc., Dalton Trans.*, in the press.
21 J. Dolansky, S. Heřmánek and R. Zahradnik, *Collect. Czech. Chem. Commun.*, 1981, **46**, 2479.
22 S. Heřmánek, T. Jelínek, J. Plešek, B. Štíbr, J. Fusek and F. Mareš, in *Boron Chemistry (IMEBORON 6)*, ed. S. Heřmánek, World Scientific Publishing Co., Singapore, 1987, pp. 26–73; S. Heřmánek, *Chem. Rev.*, 1992, **92**, 325.
23 O. W. Howarth, M. J. Jasztal, J. G. Taylor and M. G. H. Wallbridge, *Polyhedron*, 1985, **4**, 1461.
24 J. Bould, N. N. Greenwood and J. D. Kennedy, *J. Chem. Soc., Dalton Trans.*, 1984, 2477.
25 Faridoon, O. Ni Dhubhghaill, T. R. Spalding, G. Ferguson, B. Kaittner, X. L. R. Fontaine and J. D. Kennedy, *J. Chem. Soc., Dalton Trans.*, 1989, 1657.
26 S. Heřmánek, T. Jelínek, J. Plešek, B. Štíbr and J. Fusek, *J. Chem. Soc., Chem. Commun.*, 1987, 927.
27 S. Heřmánek, T. Jelínek, J. Plešek, B. Štíbr and J. Fusek, *Collect. Czech. Chem. Commun.*, 1988, **53**, 2742.
28 M. A. Beckett, M. Bown, X. L. R. Fontaine, N. N. Greenwood, J. D. Kennedy and M. Thornton-Pett, *J. Chem. Soc., Dalton Trans.*, 1986, 1969.
29 X. L. R. Fontaine and J. D. Kennedy, *J. Chem. Soc., Dalton Trans.*, 1987, 1573.
30 X. L. R. Fontaine, H. Fowkes, N. N. Greenwood, J. D. Kennedy and M. Thornton-Pett, *J. Chem. Soc., Dalton Trans.*, 1987, 1431.
31 M. Bown, X. L. R. Fontaine and J. D. Kennedy, *J. Chem. Soc., Dalton Trans.*, 1986, 1467.
32 X. L. R. Fontaine, N. N. Greenwood, J. D. Kennedy, P. MacKinnon and M. Thornton-Pett, *J. Chem. Soc., Dalton Trans.*, 1986, 2809.
33 M. Bown, X. L. R. Fontaine, N. N. Greenwood and J. D. Kennedy, *Z. Anorg. Allg. Chem.*, 1991, **602**, 17.
34 J. D. Kennedy, B. Štíbr, T. Jelínek, X. L. R. Fontaine and M. Thornton-Pett, *Collect. Czech. Chem. Commun.*, in the press.
35 R. Ugo, F. Canati and G. LaMonica, *Inorg. Synth.*, 1968, **11**, 105.
36 B. Štíbr, J. Plešek and S. Heřmánek, *Collect. Czech. Chem. Commun.*, 1973, **38**, 338.
37 B. Štíbr, J. Plešek and S. Heřmánek, *Inorg. Synth.*, 1983, **22**, 237.
38 M. Bown, J. Plešek, K. Baše, B. Štíbr, X. L. R. Fontaine, N. N. Greenwood and J. D. Kennedy, *Magn. Reson. Chem.*, 1989, **29**, 947.
39 X. L. R. Fontaine, J. D. Kennedy, M. McGrath and T. R. Spalding, *Magn. Reson. Chem.*, 1991, **29**, 711.
40 S. Heřmánek, J. Fusek, B. Štíbr, J. Plešek and T. Jelínek, *Polyhedron*, 1986, **5**, 1873.
41 W. McFarlane, *Proc. R. Soc. London, Ser. A*, 1968, **306**, 185.
42 A. Modinos and P. Woodward, *J. Chem. Soc., Dalton Trans.*, 1974, 2065.
43 N. Walker and D. Stuart, *Acta Crystallogr., Sect. A*, 1983, **39**, 158.
44 G. M. Sheldrick, SHELX 76, Program System for X-Ray Structure Determination, University of Cambridge, Cambridge, 1976.

Received 28*th August* 1992; *Paper* 2/04649K